Supporting Information
For

HIO_x-$IONO_2$ Dynamics at the Air-Water Interface: Revealing the Existence of a Halogen Bond at the Atmospheric Aerosol Surface

Manoj Kumar,[1] Tarek Trabelsi,[1] Juan Carlos Gómez Martín,[2] Alfonso Saiz-Lopez,[3] Joseph S. Francisco[1,*]

[1]Department of Earth and Environmental Science and Department of Chemistry, University of Pennsylvania, Philadelphia, Pennsylvania, USA 19104-6243.

[2]Solar System Department, Andalusian Institute for Astrophysics, CSIC, Granada, Spain, 18008.

[3]Department of Atmospheric Chemistry and Climate, Institute of Physical Chemistry Rocasolano, CSIC, Madrid, Spain, 28006.

*Email: frjoseph@sas.upenn.edu

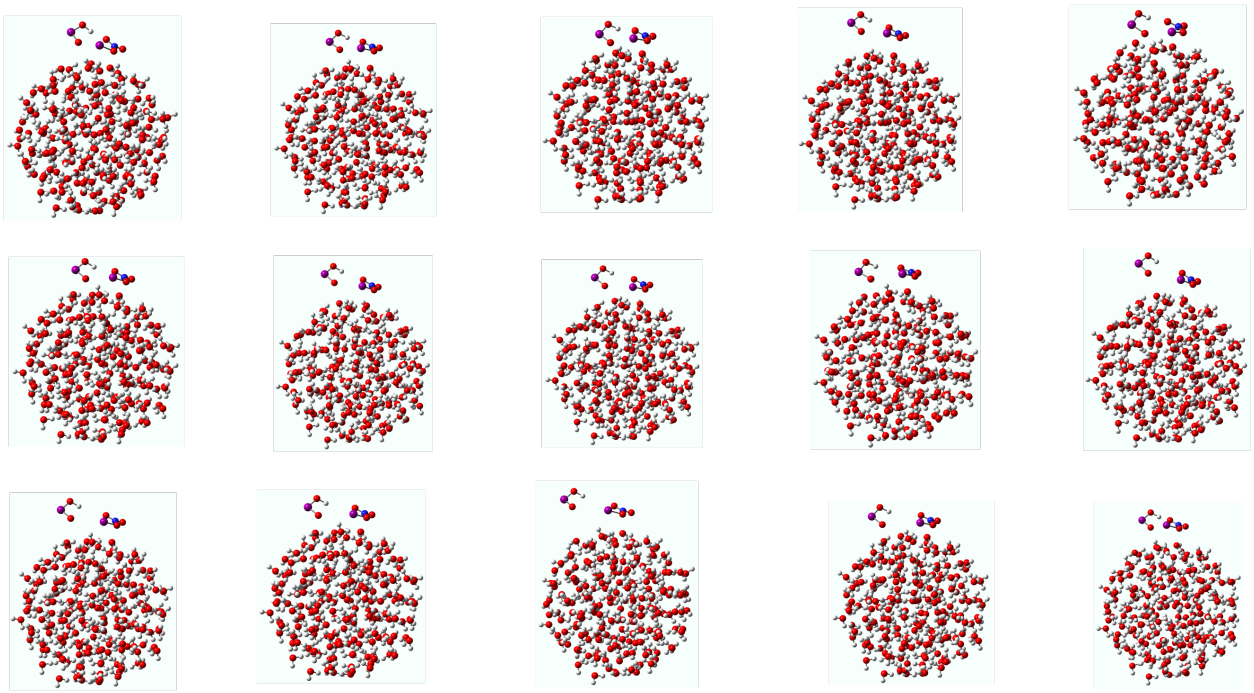

Figure S1. Initial configurations of the $HIO_2 \cdots IONO_2$ complex at the air-water interface represented by a water droplet of 191 water molecules.

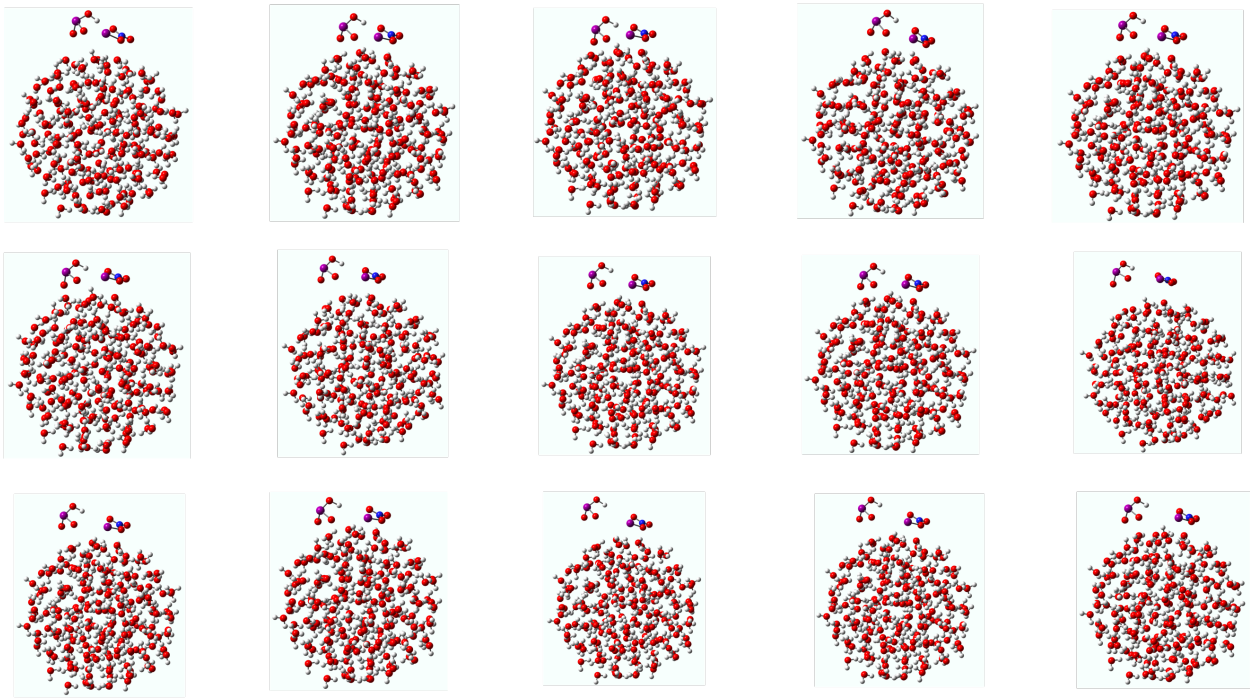

Figure S2. Initial configurations of the $HIO_3 \cdots IONO_2$ complex at the air-water interface represented by a water droplet of 191 water molecules.

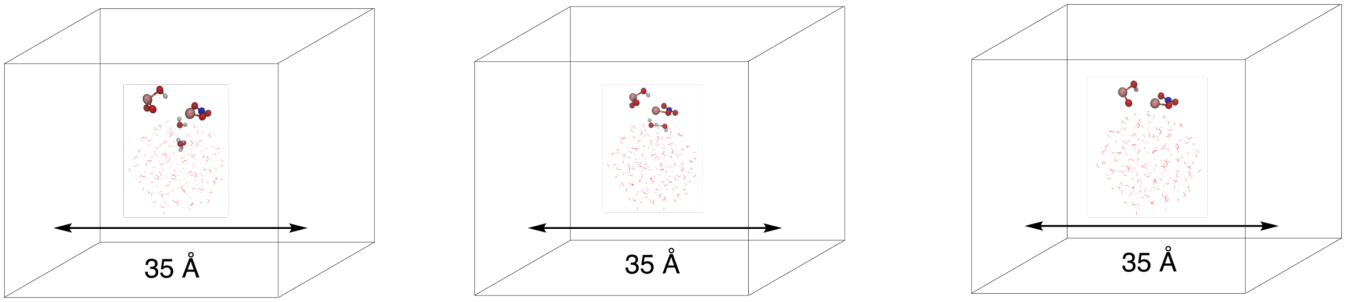

Figure S3. Initial configurations of the $HIO_3\cdots IONO_2$ and $HIO_2\cdots IONO_2$ complexes at the air-water interface represented by a water droplet of 191 water molecules. The complexes as well as key solvent molecules are shown in ball-stick representation whereas rest of the water droplet is shown in line representation. Note that the left most initial configuration of the interface-bound $HIO_3\cdots IONO_2$ corresponds to halogen bond formation in which oxygen of HIO_3 interacting with I of $IONO_2$ does not undergo protonation whereas the middle panel represents that interface-bound $HIO_3\cdots IONO_2$ configuration in which oxygen of HIO_3 interacting with I of $IONO_2$ undergoes protonation.

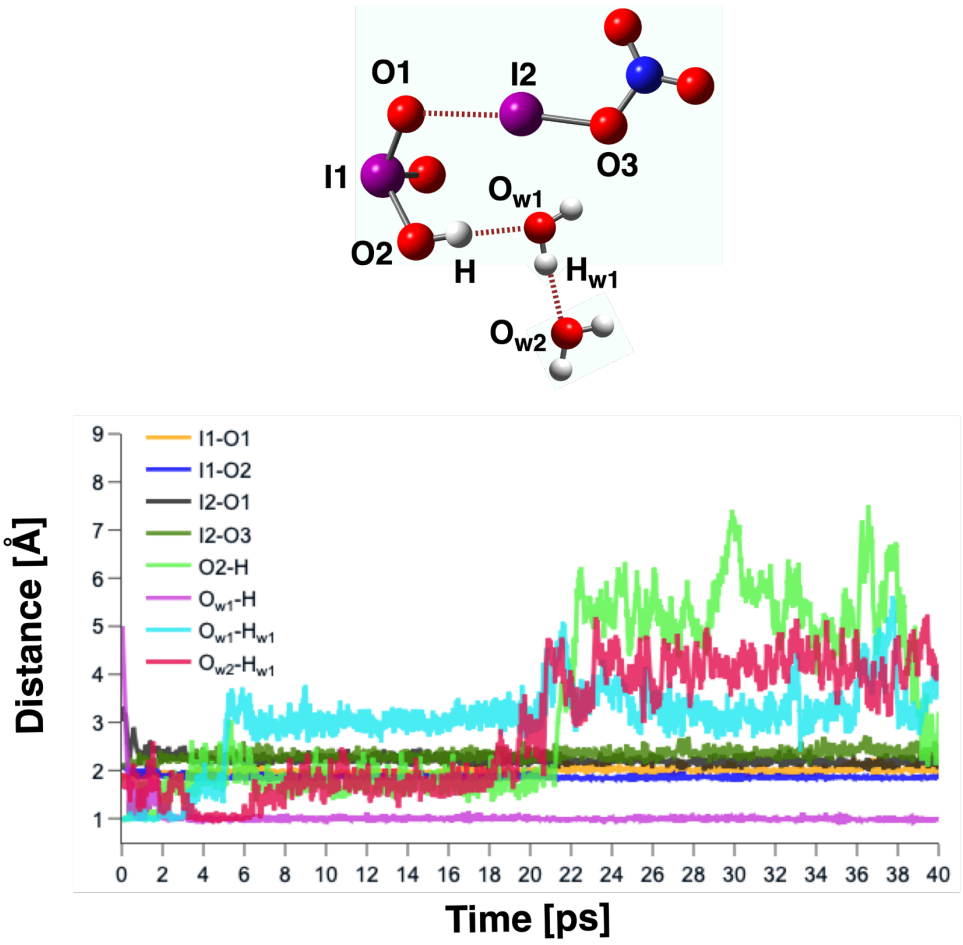

Figure S4. Time evolution of key bond distances involved in the $HIO_3\cdots IONO_2$ interaction en route to halogen bond formation. This figure describes the dominant mechanistic channel that leads to halogen bond formation between HIO_3 and $IONO_2$ at the air-water interface. The ball-stick representation of $HIO_3\cdots IONO_2$ describes the numbering scheme used in the figure.

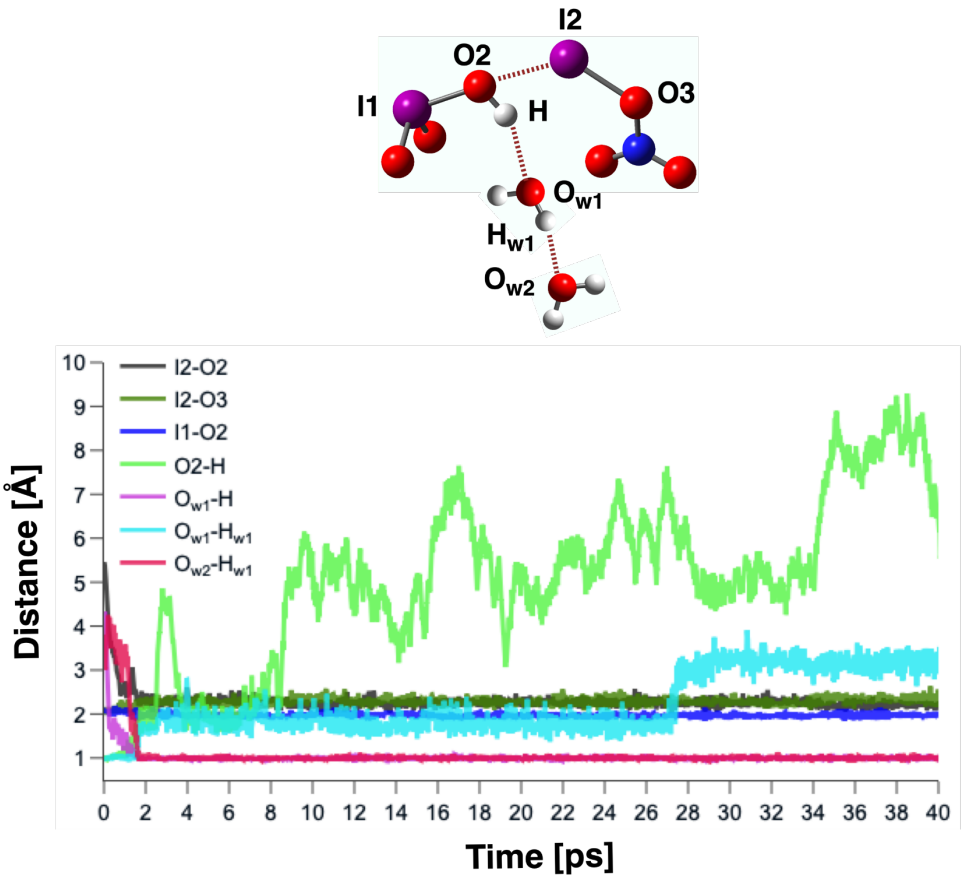

Figure S5. Time evolution of key bond distances involved in the HIO_3···$IONO_2$ interaction en route to halogen bond formation. This figure describes the minor mechanistic channel that leads to halogen bond formation between HIO_3 and $IONO_2$ at the air-water interface. The ball-stick representation of HIO_3···$IONO_2$ describes the numbering scheme used in the figure.

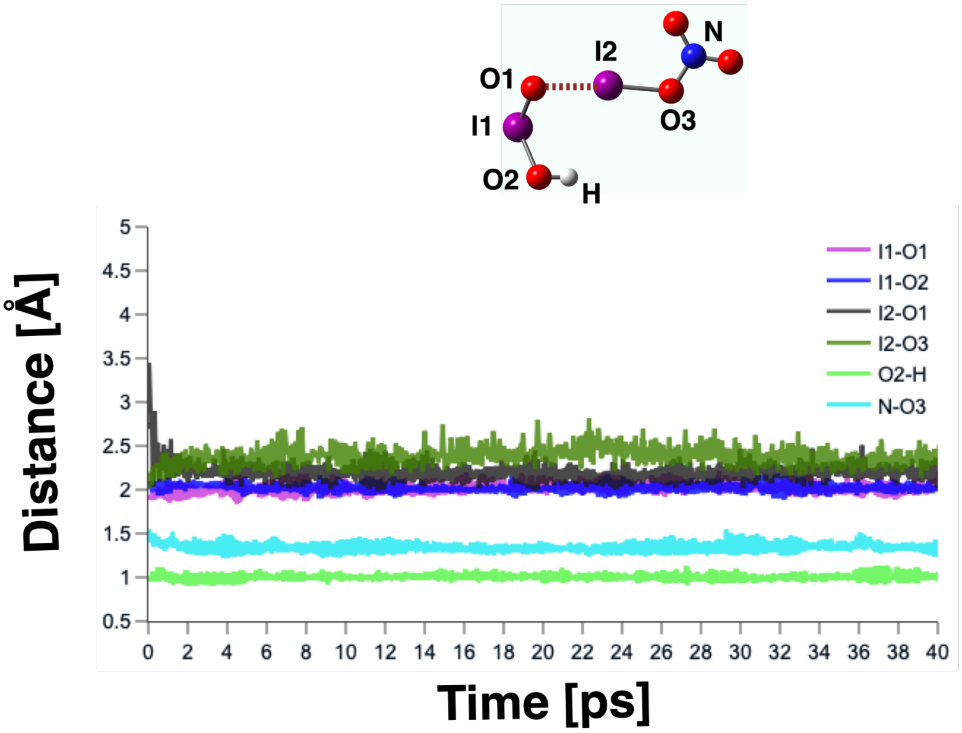

Figure S6. Time evolution of key bond distances involved in the $HIO_2\cdots IONO_2$ interaction en route to halogen bond formation. The ball-stick representation of $HIO_2\cdots IONO_2$ describes the numbering scheme used in the figure.

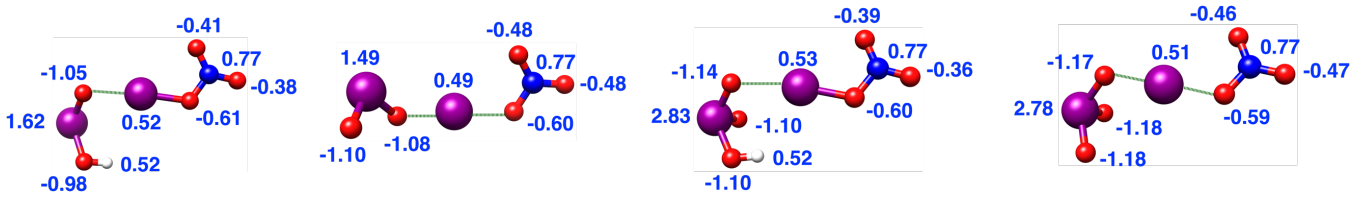

Figure S7. The M06-2X/aug-cc-pVDZ+LANL2DZ calculated natural bond orbital charge distribution in $HIO_2\cdots IONO_2$, $IO_2^-\cdots IONO_2$, $HIO_3\cdots IONO_2$ and $IO_3^-\cdots IONO_2$ complexes, respectively. Iodine is shown in magenta, oxygen in red, nitrogen in blue, and hydrogen in white.

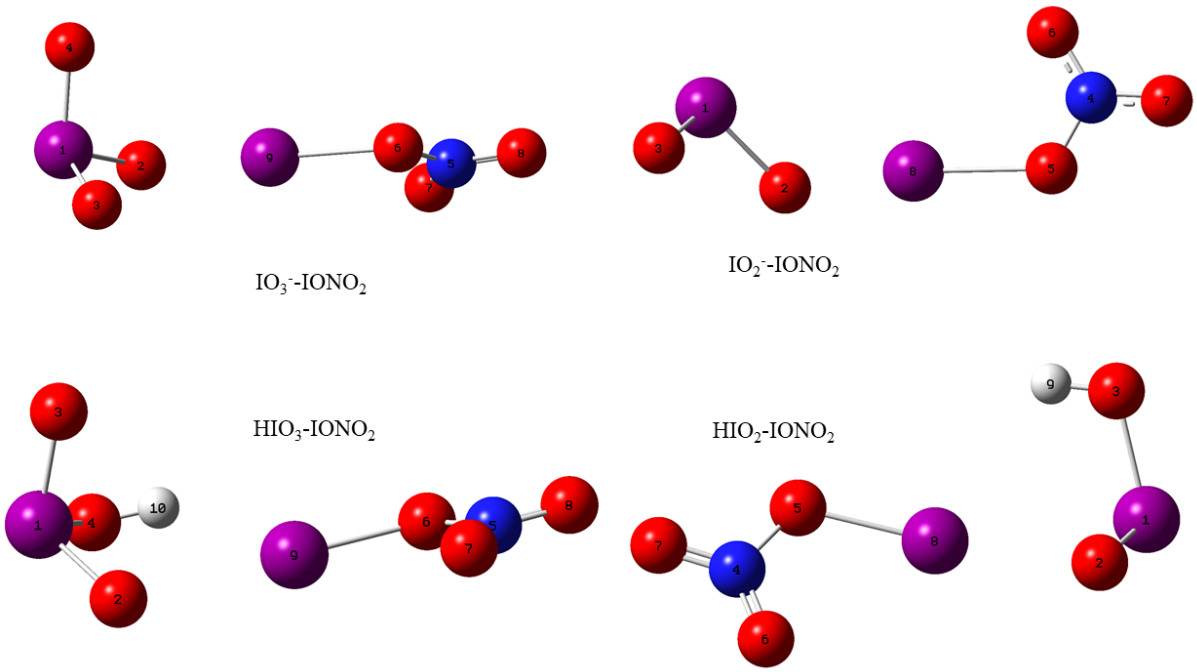

Figure S8. Numbering scheme of iodine species used in the discussion of frequency results.

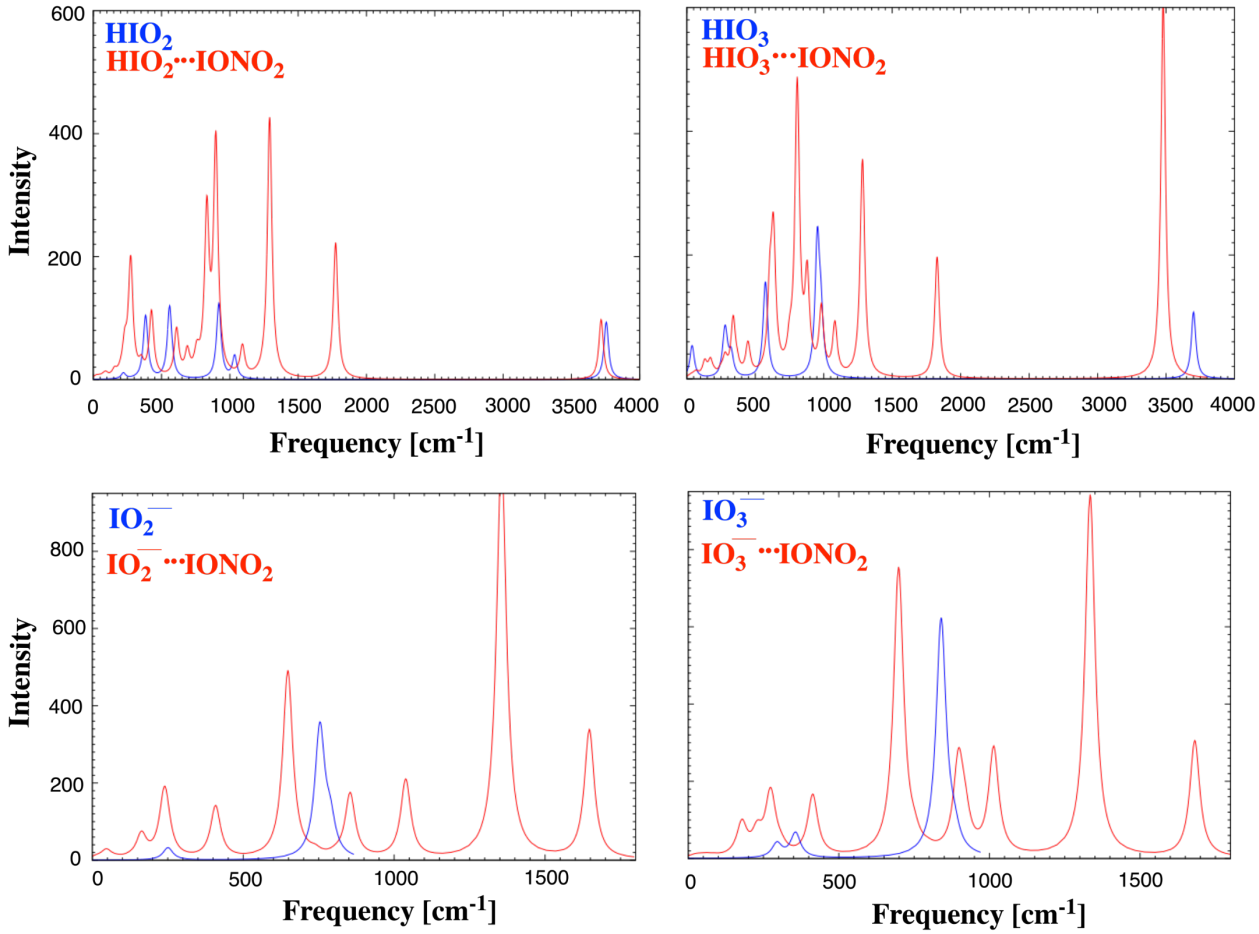

Figure S9. The MP2/aug-cc-pVDZ+LANL2DZ calculated spectra of free HIO_2, IO_2^-, HIO_3 and IO_3^- as well as their $IONO_2$ complexes. The blue curves represent the spectra of iodine species before complexation and the red ones show their spectra after complexation. See also **Table S1**.

Table S1. M06-2X/aug-cc-pVDZ+LANL2DZ optimized geometries of key species involved in the $HIO_2\cdots IONO_2$, $IO_2^-\cdots IONO_2$, $HIO_3\cdots IONO_2$ and $IO_3^-\cdots IONO_2$ complexes, as well as those of I_2O_2 and I_2O_3 respectively.

HIO_2

I	0.091717	-0.272203	0.005263
O	-1.656390	0.596994	-0.113516
H	-1.875321	0.997215	0.739960
O	1.283179	1.081700	-0.013846

IO_2^-

I	0.000000	0.244056	0.000000
O	1.540115	-0.808438	0.000000
O	-1.540115	-0.808433	0.000000

HIO_3

I	-0.252391	0.060145	0.000000
O	0.496217	-1.702599	0.000000
H	1.467532	-1.665057	0.000000
O	0.496217	0.756135	1.417565
O	0.496217	0.756135	-1.417565

IO_3^-

I	0.000366	-0.000168	-0.214379
O	-1.115500	-1.210641	0.473191
O	-0.493287	1.570254	0.472923
O	1.606362	-0.358502	0.474146

$IONO_2$

N	1.859211	0.070090	0.000027
O	0.776712	-0.813773	-0.000155
O	1.635516	1.246615	-0.000063
O	2.900777	-0.516291	0.000097
I	-1.047519	0.003339	0.000015

I_2O_2

I	1.574526	-0.169897	-0.084719
O	-0.136250	-0.877822	0.592008
O	1.492482	1.594620	0.278043
I	-1.779240	0.061702	-0.046610

I_2O_3

I	1.444789	0.376894	0.000000
O	1.444789	-0.644631	1.416924
O	1.444789	-0.644631	-1.416924
O	-0.367294	1.034359	0.000000
I	-1.825511	-0.338418	0.000000

$HIO_2\cdots IONO_2$

I	2.547354	-0.079210	-0.284158
O	1.292862	-1.065609	0.606160
O	2.377902	1.647650	0.554901
N	-3.819176	0.127356	-0.270103
O	-2.695301	0.860360	-0.070715
O	-3.738433	-1.076085	-0.225110
O	-4.799139	0.795018	-0.476416
I	-0.930670	-0.151741	0.256190
H	1.546845	2.058230	0.262495

$IO_2^-\cdots IONO_2$

I	-2.428124	0.381283	-0.165647
O	-1.152374	-1.011354	-0.448056
O	-3.177224	0.147024	1.484573
N	3.742085	0.656993	0.092981
O	3.111975	-0.445671	0.361313
O	3.117557	1.616226	-0.341763
O	4.949561	0.666378	0.298422
I	0.900000	-0.614864	-0.051085

$HIO_3\cdots IONO_2$

I	-2.577281	-0.088924	0.023173
O	-1.273183	-0.956098	-0.796404
O	-2.275966	-0.179312	1.735782
O	-2.102537	1.706514	-0.383153
N	4.012513	0.032991	0.275986
O	2.916164	0.836219	0.081778
O	3.861194	-1.160153	0.238339
O	5.018630	0.658236	0.465088
I	1.141869	-0.087420	-0.258987
H	-1.165164	1.872007	-0.165209

$IO_3^-\cdots IONO_2$

I	-2.509433	-0.080277	-0.022594
O	-0.989412	-0.556858	-0.946779
O	-2.354934	-0.873206	1.544977
O	-2.348467	1.655655	0.241384
N	4.037549	-0.056750	0.273526
O	3.026021	0.774994	0.278691
O	3.857545	-1.218237	-0.051680
O	5.116381	0.411179	0.602775
I	1.024151	0.058561	-0.265512

Table S2. MP2/aug-cc-pVDZ+LANL2DZ optimized geometries of key species involved in the $HIO_2\cdots IONO_2$, $IO_2^-\cdots IONO_2$, $HIO_3\cdots IONO_2$ and $IO_3^-\cdots IONO_2$ complexes, respectively.

HIO_2

I	0.10186400	-0.24595800	0.01527200
O	-1.68125200	0.60396700	-0.12306400
H	-1.89452100	0.98099800	0.74846600
O	1.31709400	1.06470000	-0.02281300

IO_2^-

I	0.00000100	0.23561100	0.00000000
O	1.52882800	-0.80421500	0.00000000
O	-1.52882900	-0.80421100	0.00000000

HIO_3

I	-0.25289600	0.07254600	0.00002900
O	0.49647400	-1.72904400	0.00013700
H	1.47273100	-1.66871500	-0.00023600
O	0.49365400	0.76506200	1.42414900
O	0.49383000	0.76491000	-1.42408000

IO_3^-

I	-0.00026200	0.00011800	-0.21615100
O	-1.11826900	-1.21522600	0.47372100
O	-0.49438400	1.57597100	0.47338300
O	1.61085700	-0.35991900	0.47492800

$IONO_2$

N	1.87448400	0.08364400	-0.00005300
O	0.75178800	-0.84046600	-0.00008000
O	1.63838900	1.27223200	-0.00001500
O	2.92223200	-0.52787900	0.00008900
I	-1.06219500	0.00244900	-0.00002000

$HIO_2\cdots IONO_2$

I	2.32843900	-0.32384400	0.13729100
O	1.28702500	-0.57913500	1.59973400
O	2.10548300	1.55647300	-0.30030000
N	-3.52133400	0.33996600	-0.43484800
O	-3.14458100	-0.28079700	0.74225300
O	-2.64939500	0.77305200	-1.18151400
O	-4.73464800	0.37850100	-0.58942600
I	-1.13065700	-0.40841300	1.12330800
H	1.24191000	1.66016600	-0.74325300

$IO_2^-\cdots IONO_2$

I	-2.51396700	0.37233700	-0.10790200
O	-1.18125800	-0.94008300	-0.54477000
O	-3.19313400	0.02676800	1.53431000
N	3.78093800	0.65024600	0.08662600
O	3.06809100	-0.38495600	0.47317800
O	3.23507100	1.56835500	-0.55172600
O	4.98787300	0.64140700	0.39537600
I	0.87984100	-0.53806000	-0.05435300

$HIO_3\cdots IONO_2$

I	-2.61470700	0.06349700	0.00927600
O	-1.40519200	-0.85649000	-0.90802600
O	-2.62326100	-0.50451400	1.65710000
O	-1.66784500	1.73924800	0.12026400
N	3.91002900	0.14054800	0.31719300
O	2.99197800	0.72046500	-0.61002900
O	3.53967800	-0.81606700	0.97166600
O	4.97946200	0.72012500	0.30446500
I	1.15224300	-0.10213300	-0.67188400
H	-0.70614600	1.52938100	0.02636900

$IO_3^-\cdots IONO_2$

I	-2.56248800	-0.12332500	-0.02488700
O	-0.96873100	-0.59311300	-0.85026900
O	-2.39872100	-0.66088100	1.65153700
O	-2.58297700	1.64494700	-0.01579200
N	4.10885800	-0.06410400	0.23004300
O	3.02745900	0.62050900	0.59024500
O	3.98766100	-1.05982100	-0.49684600
O	5.18668700	0.36900200	0.66726000
I	1.06165300	-0.01815300	-0.09650300

Table S3. The CCSD(T)/aug-cc-pVTZ + LANL2DZ //M062X/aug-cc-pVDZ + LANL2DZ electronic energies of all Iodine species studied in this work. The M062X/aug-cc-pVDZ + LANL2DZ calculated harmonic frequencies, zero-point correction, thermal correction to Gibbs free energy and rotational constants are also given.

Iodine species	Electronic energies	Harmonic frequencies	Zero-point correction	Thermal correction to Gibbs free energy	Rotational constants
HIO_2	-162.0076923	219.12, 381.3, 605.2, 782.5, 1078.1, 3827.6	0.015705	-0.012149	14.34814, 6.69028, 4.62250
IO_2^-	-161.4453762	256.7, 676.7, 693.8	0.003707	-0.023763	17.85676, 6.66038, 4.85100
HIO_3	-237.1352677	141.7, 280.3, 309.9, 329.0, 629.0, 877.8, 910.6, 1003.4, 3780.7	0.018824	-0.010592	5.91929, 5.63580, 3.80381
IO_3^-	-236.6116925	296.1, 298.5, 349.6, 807.1, 824.8, 826.7	0.007752	-0.020859	6.20791, 6.19792, 3.88736
$IONO_2$	-291.1322531	85.1, 210.4, 393.6, 693.0, 795.2, 802.2, 912.6, 1400.9, 1802.8	0.016165	-0.014409	12.70344, 1.35806, 1.22690
HIO_2-$IONO_2$	-453.1638313	32.8, 42.3, 64.0, 85.2, 93.5, 157.1, 201.3, 231.3, 276.7, 354.0, 423.6, 643.1, 728.0, 741.6, 789.8, 826.5, 989.0, 1138.9, 1404.9, 1748.0, 3775.3	0.033596	-0.007142	3.48784, 0.25303, 0.24382
IO_2^--$IONO_2$	-452.6602735	14.9, 51.8, 64.0, 83.4, 138.0, 159.4, 173.3, 238.3, 263.3, 438.5, 671.2, 737.8, 744.4, 760.3, 855.7, 1097.4, 1414.5, 1631.0	0.021727	-0.019274	2.68378, 0.25559, 0.24412
HIO_3-$IONO_2$	-528.2852959	33.8, 41.3, 48.9, 63.5, 80.3, 139.8, 156.3, 211.5, 217.5, 289.2, 340.6, 345.6, 375.4, 647.5, 720.2, 797.0, 817.6, 835.7, 907.4, 957.5, 1036.0, 1404.9, 1774.3, 3708.8	0.036338	-0.006158	2.78404, 0.22317, 0.22006
IO_3^--$IONO_2$	-527.8019476	1.5, 34.4, 46.5, 67.6, 88.4, 160.4, 180.6, 240.0, 272.6, 294.4, 313.4, 427.9, 719.5, 736.9, 771.5, 847.0, 848.7, 871.1, 1078.3, 1412.8, 1655.3	0.025217	-0.019557	2.99350, 0.22723, 0.22442

Table S4. M062X/aug-cc-pVDZ + LANL2DZ and MP2/aug-cc-pVDZ + LANL2DZ harmonic vibrational frequencies (ω_i in cm^{-1}) of all Iodine species studied in this work. Intensities are given in parentheses.

M062X/aug-cc-pVDZ + LANL2DZ									
	HIO_3-$IONO_2$	HIO_2-$IONO_2$	IO_3^--$IONO_2$	IO_2^--$IONO_2$	HIO_3	$IONO_2$	HIO_2	IO_3^-	IO_2^-
ω_1	3708 (196)	3775 (117)	1651 (481)	1631 (491)	3780 (142)	1802 (415)	3827 (123)	826 (193)	693 (150)
ω_2	1774 (424)	1747 (434)	1411 (870)	1414 (869)	1003 (54)	1400 (339)	1078 (41)	824 (191)	676 (21)
ω_3	1404 (472)	1404 (561)	1081 (267)	1097 (232)	910 (119)	912 (315)	782 (41)	806 (28)	256
ω_4	1036 (84)	1138 (68)	871 (136)	855 (13)	877 (26)	802 (13)	605 (79)	349	
ω_5	957 (406)	989 (4470	852 (12)	760 (6)	629 (116)	795 (1)	381	298	
ω_6	907 (101)	826 (13)	847 (65)	744 (87)	328	692 (30)	219	296	
ω_7	835 (149)	789 (8)	773 (96)	737 (0.6)	309	393			
ω_8	817 (14)	741 (118)	736 (1)	671 (302)	280	210			
ω_9	797 (14)	728 (16)	718 (486)	438	141	85			
ω_{10}	720 (20)	643 (52)	430	263					
ω_{11}	647 (86)	423	312	238					
ω_{12}	375	354	292	173					
ω_{13}	345	276	275	159					
ω_{14}	340	231	243	138					
ω_{15}	289	201	181	83					
ω_{16}	217	157	168	64					
ω_{17}	211	93	89	51					
ω_{18}	156	85	65	16					
ω_{19}	139	64	48						
ω_{20}	80	42	36						
ω_{21}	63	32	20						
ω_{22}	48								
ω_{23}	41								
ω_{24}	33								
MP2/aug-cc-pVDZ + LANL2DZ									
ω_1	3479(600)	3717(100)	1681(300)	1646(333)	3701(108)	1853(192)	3755(90)	882(44)	788(80)
ω_2	1828(200)	1774(220)	1334(940)	1355(999)	979(80)	1282(272)	1035(40)	839(307)	753(330)
ω_3	1282(350)	1291(424)	1014(274)	1038(200)	956(16)	786(274)	919(112)	839(307)	250(30)
ω_4	1081(81)	1092(50)	918(75)	854(165)	953(200)	745(6)	558(118)	356(64)	
ω_5	982(104)	896(380)	897(230)	806(6)	573(155)	735(6)	383	294	
ω_6	879(150)	831(260)	796(5)	737	324	576(230)	220	294	
ω_7	806(466)	767(6)	750(25)	714	283	375			
ω_8	752(20)	756(27)	713(2)	647	273	194			
ω_9	747(15)	688	698(743)	408	38	114			
ω_{10}	632	610	413	246					
ω_{11}	606	426	308	238					
ω_{12}	446	351	280	163					
ω_{13}	368	273	272	159					
ω_{14}	339	229	228	122					
ω_{15}	279	199	178	75					
ω_{16}	248	155	160	47					
ω_{17}	200	91	86	39					
ω_{18}	172	73	63	14					
ω_{19}	131	45	44						
ω_{20}	78	23	25						
ω_{21}	63	19	4						
ω_{22}	47								
ω_{23}	28								
ω_{24}	15								